THE JOURNAL OF BIOLOGICAL CHEMISTRY
Vol. 268, No. 31, Issue of November 5, pp. 23087-23092, 1993
Printed in U.S.A.

Long Range Propagation of Conformational Changes in Integrin $\alpha_{IIb}\beta_3$*

(Received for publication, April 14, 1993, and in revised form, June 30, 1993)

Xiaoping Du‡, Minyi Gu, John W. Weisel§, Chandrasekaran Nagaswami§, Joel S. Bennett§, Ron Bowditch¶, and Mark H. Ginsberg

From the Committee on Vascular Biology, The Scripps Research Institute, La Jolla, California 92037 and the §Department of Cell and Developmental Biology and Department of Medicine, University of Pennsylvania School of Medicine, Philadelphia, Pennsylvania 19104

Integrin adhesion receptors participate in two-way transfer of information across the plasma membrane. For example, cytoplasmic events, such as activation of protein kinase C, cause an increase in the fibrinogen (Fg) binding affinity of the extracellular domain of integrin $\alpha_{IIb}\beta_3$ ("inside-out signaling"). Conversely, ligand binding to $\alpha_{IIb}\beta_3$ results in the generation of intracellular signals. We used anti-LIBS2, an anti-β_3 monoclonal antibody, to understand potential mechanisms of this bidirectional signaling. Anti-LIBS2 bound to $\alpha_{IIb}\beta_3$ with low affinity (K_d = 7.4 μM), and mimicked inside-out signaling by promoting Fg binding. The affinity of anti-LIBS2 binding was increased 20-fold (K_d = 326 nM) by addition of an Fg-mimetic synthetic peptide, RGDS. Thus, anti-LIBS2 and ligands (Fg and Fg-mimetic peptides) bind cooperatively to integrin $\alpha_{IIb}\beta_3$, indicating a functional linkage between the ligand-binding site and the antibody-binding site. The anti-LIBS2-binding site was mapped by its binding to proteolytic and recombinant fragments of the β_3 subunit. The epitope was located within an 89-residue region immediately adjacent to the transmembrane domain and 400 residues carboxyl-terminal to the known ligand-binding site(s). Electron microscope images of rotary shadowed ternary complexes of Fg, anti-LIBS2, and $\alpha_{IIb}\beta_3$ revealed that the ligand-binding site and anti-LIBS2 epitope are separated by about 16 nm. This indicates that propagated long distance conformational changes can occur in $\alpha_{IIb}\beta_3$. Such changes are likely to be involved in the bidirectional signaling function of this integral membrane protein.

Integrins are cell surface receptors that mediate cell-cell and cell-matrix adhesion and in doing so transfer information across the plasma membrane. This function is exemplified by the platelet integrin $\alpha_{IIb}\beta_3$. In the normal circulation, $\alpha_{IIb}\beta_3$ on the surface of resting platelets does not bind soluble macromolecular ligands such as fibrinogen (Fg).[1] However, when platelets are exposed to appropriate agonists, the Fg binding affinity of $\alpha_{IIb}\beta_3$ is markedly increased (1, 2) probably due to a conformational change in the integrin (3, 4). Cytoplasmic signaling elements such as G proteins, Ca^{2+} mobilization, and protein kinases provoke this conformational change, which thus represents "inside-out" signal transduction (5, 6). In addition to conformational changes associated with inside-out signaling, Fg binding to $\alpha_{IIb}\beta_3$ also changes the receptor's conformation (7) and leads to platelet aggregation and secretion, tyrosine phosphorylation of intracellular proteins, and ion fluxes across the membrane (8). Thus, $\alpha_{IIb}\beta_3$ transmits information in both directions across the plasma membrane.

Changes in receptor conformation may explain the capacity of certain receptors to initiate transmembrane signals (9–13). Ligand-induced conformational changes have been documented in soluble purified receptors (13–15). Since the receptors of interest are usually integral membrane proteins, some of these experiments used detergent-solubilized receptors or soluble recombinant receptors lacking transmembrane domains. Evidence of ligand-induced conformational change *in situ* has been obtained by use of elegant but arduous proteolytic (9, 11, 16) or recombinant receptor (10) methods. Monoclonal antibodies specific for occupied conformers of cell surface receptors (anti-LIBS) (17) have also provided a method to document ligand-induced conformational changes *in situ*.

Anti-$\alpha_{IIb}\beta_3$ LIBS antibodies, by definition (17), detect ligand-induced conformational changes. In addition, certain anti-LIBS increase the Fg binding affinity of $\alpha_{IIb}\beta_3$ (18, 19). Antibody-"activated" and physiologically activated $\alpha_{IIb}\beta_3$ bind Fg with similar affinities (1, 18, 19), bind a similar spectrum of ligands other than Fg (4, 18, 20, 21), and are blocked by the same synthetic peptides and monoclonal antibodies (4, 18, 19). Moreover, point mutations in $\alpha_{IIb}\beta_3$ that abrogate Fg binding to $\alpha_{IIb}\beta_3$ on stimulated platelets, also block Fg binding to the anti-LIBS-activated receptor (22, 23). Thus, anti-LIBS "activation" of $\alpha_{IIb}\beta_3$ mimics physiologic inside-out signaling. We have characterized an anti-$\alpha_{IIb}\beta_3$ LIBS with these properties and mapped its epitope in relation to the $\alpha_{IIb}\beta_3$ ligand-binding site. The anti-LIBS epitope was 16 nm from the ligand-binding site and near the membrane-spanning domain. Our results show that integrin $\alpha_{IIb}\beta_3$ can undergo propagated long distance conformational changes. Such changes are likely to be involved in bidirectional signaling by this receptor.

EXPERIMENTAL PROCEDURES

Materials—Human Fg was purified from plasma as previously described (24). Anti-LIBS monoclonal antibodies were prepared and characterized as previously described (4). Fab fragments were prepared by digestion with immobilized papain (Pierce Chemical Co.) under conditions recommended by the manufacturer. The undigested

* The work described herein was supported by Grants AR-27214, HL-28235, HL-30954, HL-40387, and HL-48728 from the National Institutes of Health. This is publication 7947-CVB from the Scripps Research Institute. The costs of publication of this article were defrayed in part by the payment of page charges. This article must therefore be hereby marked "*advertisement*" in accordance with 18 U.S.C. Section 1734 solely to indicate this fact.

‡ Postdoctoral fellow of the California Heart Association. To whom correspondence should be addressed. Tel.: 619-554-7115; Fax: 619-554-6403.

¶ Postdoctoral fellow of the California Heart Association.

[1] The abbreviations used are: Fg, fibrinogen; BSA, bovine serum albumin; IPTG, isopropyl-β-D-thiogalactopyranoside; LIBS, ligand-induced binding site; PGE_1, prostaglandin E_1; MBP, maltose-binding protein.

IgG and Fc fragments were removed by repeated absorption using Protein A-conjugated Sepharose 4B (Pharmacia LKB Biotechnology Inc.). mAb15 is a monoclonal antibody against β_3 with no known functional effect (4). Oligonucleotides used in polymerase chain reactions and sequencing were synthesized using a 391 PCR-mate nucleotide synthesizer (Applied Biosystems, Foster City, CA). Restriction enzymes were purchased from Boehringer Mannheim. The peptide Arg-Gly-Asp-Ser (RGDS) was purchased from Peninsula Laboratories, Belmont, CA. Bovine serum albumin (BSA), chymotrypsin, phenylmethylsulfonyl fluoride, prostaglandin E_1 (PGE_1), and isopropyl-β-D-thiogalactopyranoside (IPTG) were purchased from Sigma.

Anti-LIBS2 and Fg Binding to Platelets—Platelets, obtained from fresh ACD-anticoagulated human blood, were separated from plasma proteins by gel filtration using a Sepharose 2B column equilibrated with modified Tyrode's buffer (5 mM HEPES, 148 mM NaCl, 2.5 mM KCl, 12 mM $NaHCO_3$, 5.5 mM glucose, and 1 mg/ml BSA, pH 7.4) containing 250 ng/ml PGE_1 (25). The gel-filtered platelets were suspended in the modified Tyrode's buffer containing 1 mM $CaCl_2$ and 1 mM $MgCl_2$ and various concentrations of ^{125}I-labeled anti-LIBS2 were added. After incubating at 22 °C for 1 h, bound anti-LIBS2 was separated from the free by sedimenting the platelets through a layer of 20% sucrose. Fg binding assays were performed under the same conditions as the antibody binding assays except that various concentrations of unlabeled anti-LIBS2 were added together with 300 nM of labeled Fg. Iodination of the antibodies and Fg was performed as previously described (4).

Binding of Anti-LIBS2 to Chymotryptic Fragments of β_3—Gel-filtered platelets suspended in 0.01 M HEPES, 5 mM EDTA, 0.15 M NaCl, pH 7.4, were incubated with 0.5 mg/ml α-chymotrypsin at 37 °C for 0, 1, and 4 h after which the reaction was stopped by adding 2 mM phenylmethylsulfonyl fluoride. The platelets were then solubilized in sample buffer (26) containing 2% SDS and the dissolved platelet proteins were separated by electrophoresis on a 7.5% SDS-polyacrylamide gel. The separated proteins were transferred to nitrocellulose paper (27) and stained with anti-LIBS2 IgG and control antibodies (28).

Localization of the Anti-LIBS2 Epitope Using a β_3 cDNA Fragment Library—A 2.6-kilobase full-length β_3 cDNA (29) was randomly digested with DNase I (Boehringer Mannheim) (enzyme/substrate ratio 1:10,000) for 30 min. The resulting DNA fragments were blunt-ended with T4 DNA polymerase, ligated to *Eco*RI-*Not*I linkers and then inserted into the *Eco*RI site of λgt11. The λgt11 library was then screened by plating *Escherichia coli* Y1090 cells infected with the β_3 fragment-containing phages, and transferring the resulting plaques to IPTG-treated nitrocellulose membranes. The membranes were sequentially incubated with anti-LIBS2 antibody, biotinylated rabbit anti-mouse IgG, and a peroxidase-conjugated avidin-biotin complex (Vector Laboratories, Burlingame, CA). Positive clones were visualized by adding the substrate, 4-chloronaphthal. Positive insert fragments were amplified by polymerase chain reaction using the λgt11 forward primer GGTGGCGACGACTCCTGGAGCCCG and a reverse primer TTGACACCAGACCAACTGGTAATG, and cloned into the TA vector (Invitrogen, San Diego, CA). DNA sequences were determined with a modification of the standard dideoxy nucleotide termination method (30) (Sequenase kit, U. S. Biochemical, Cleveland, OH).

Cloning in pMALcRI Vector and Mutagenesis—The cDNA fragments containing the LIBS2 epitope were separated from the TA vector by digestion with *Eco*RI and ligated to the *Eco*RI-digested pMALcRI vector (New England Biolabs, Beverly, MA). After verification of their DNA sequences, the constructs were used to transform *E. coli* αDH52 cells. The expression of the maltose-binding protein (MBP)-LIBS2 fusion protein in *E. coli* αDH52 cells was induced by addition of 0.3 mM IPTG. Cells expressing the fusion proteins were solubilized in SDS sample buffer (31), and the dissolved proteins were analyzed by SDS-polyacrylamide gel electrophoresis and immunoblotting with anti-LIBS2 IgG. The MBP-LIBS2 fusion protein was purified by affinity chromatography on an amylose column (New England Biolabs) using conditions recommended by the manufacturer. Truncated LIBS2 DNA fragments of various lengths and containing point mutations were made by using the polymerase chain reaction (32).

Electron Microscopy of Rotary Shadowed Specimens—Purified integrin $\alpha_{IIb}\beta_3$ was prepared as previously described (33). $\alpha_{IIb}\beta_3$ in 0.01 M HEPES, 0.15 M NaCl, 1 mM $CaCl_2$, 1 mM $MgCl_2$, 25 mM octyl-β-D-glucopyranoside, 0.1% NaN_3, pH 7.4, was incubated with anti-LIBS2 IgG or Fg at 37 °C for 1.5 h before the sample was prepared for electron microscopy. Most experiments were carried out with $\alpha_{IIb}\beta_3$ and antibodies at molar ratios of 1:1, 2:1, 1:2. Samples of the complexes were diluted into 0.05 M ammonium formate, pH 7.4, and 35–70% glycerol, quickly sprayed onto freshly cleaved mica and shadowed with tungsten in a vacuum evaporator (Denton Vacuum Co., Cherry Hill, NJ) (34). Specimens were examined in a Phillips 400 electron microscope at 80 KV.

Other Methods—Peptides were synthesized as previously described (35, 36). Synthetic peptides were coated onto microtiter well by adding 50 μl of a 0.01 M $NaHCO_3$, pH 8.0, containing 2.5 nmol of peptide and incubating at 4 °C for 20 h. After washing, 100 μl of a 100 nM ^{125}I-labeled anti-LIBS2 solution was added to peptide-coated wells and incubated at 22 °C for 2 h. The bound radioactivity was estimated following three additional washes. Purified $\alpha_{IIb}\beta_3$ was diluted to 80 nM in 0.01 M HEPES, 0.15 M NaCl, 1 mM $CaCl_2$, 1 mM $MgCl_2$, pH 7.4, and 50 μl of this solution was used to coat microtiter wells as described above. The effects of peptides on anti-LIBS2 binding to $\alpha_{IIb}\beta_3$ were tested by incubating 50 μl of ^{125}I-labeled anti-LIBS2 (50 nM) in $\alpha_{IIb}\beta_3$-coated wells in the presence of 2–5 mM peptide. The effects of anti-LIBS2 on Fg binding to solubilized $\alpha_{IIb}\beta_3$ were assessed as previously described (4).

RESULTS

Functional Linkage between the Ligand-binding Site and Anti-LIBS2-binding Site—We first examined the relationship between the binding of anti-LIBS2 and adhesive ligands to $\alpha_{IIb}\beta_3$ on intact platelets. Fab fragments of anti-LIBS2 bound to $\alpha_{IIb}\beta_3$ with low affinity (K_d = 7400 ± 1600 nM, n = 3) (Fig. 1*A*). Addition of RGDS, a Fg-related peptide that binds to unactivated $\alpha_{IIb}\beta_3$ (37), increased the affinity of anti-LIBS2 Fab binding by 20-fold (K_d = 326 ± 24 nM, F = 41, $p < 0.0001$, n = 3). On the other hand, the concentration of anti-LIBS2-binding sites in the presence and absence of RGDS were 7.9 ± 1.5 and 10.8 ± 3.25 nM, respectively (19,000 and 26,000 molecules/platelet), a statistically insignificant difference (F = 0.04. p = 0.961). These data indicate that the RGDS peptide induced a change in the conformation or environment of the anti-LIBS2-binding site.

Next, we examined the effect of anti-LIBS2 on Fg binding to intact platelets. Anti-LIBS2 stimulated Fg binding to the platelets in a concentration-dependent manner (Fig. 1*B*). This effect was seen at anti-LIBS2 concentrations that correspond to the lower affinity interaction of the antibody with $\alpha_{IIb}\beta_3$ (*cf.* Fig. 1*A*). Thus, the anti-LIBS2 concentration required for half-maximal induction of Fg binding (8 μM) was approximately equal to its K_d (7.4 μM) for binding to $\alpha_{IIb}\beta_3$ in the absence of RGDS. In addition, anti-LIBS2 also stimulated Fg binding to purified soluble $\alpha_{IIb}\beta_3$ (not shown). These data indicate that there is cooperativity between the anti-LIBS2-binding site and the ligand-binding site in $\alpha_{IIb}\beta_3$. Consequently, ligand binding promotes anti-LIBS2 binding and anti-LIBS2 enhances ligand binding.

The Anti-LIBS2-binding Site Is Separable from the Ligand-binding Site—One possible explanation for the cooperativity between anti-LIBS2 and Fg binding is that their binding sites may be in proximity. To test this possibility, $\alpha_{IIb}\beta_3$ was digested with chymotrypsin, yielding a 66-kDa fragment of β_3. This β_3 fragment lacks residues 101 to 378 (38), a region that contains two known ligand-binding sites (39, 40). By immunoblotting, anti-LIBS2 reacted with both intact β_3 and the 66-kDa chymotryptic fragment (Fig. 2). Since the 66-kDa fragment lacks the ligand-binding domain, these data establish that the anti-LIBS2 epitope and the ligand-binding site are distinct structures.

Localization of Anti-LIBS2-binding Site—To localize more precisely the anti-LIBS2-binding site, a λgt11 expression library was constructed with random fragments of β_3 cDNA. Phage-containing DNA fragments encoding the anti-LIBS2 epitope were identified by immunostaining of plaques trans-

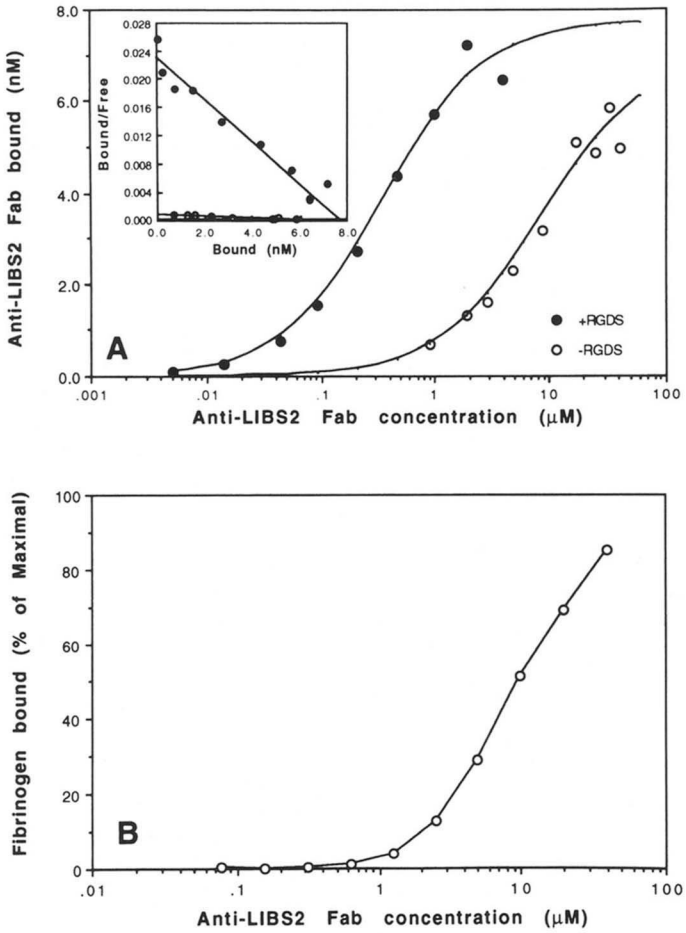

FIG. 1. **Anti-LIBS2 Fab fragment binding to platelets and anti-LIBS2-induced Fg binding.** *A*, human platelets (2.5×10^8/ml) were incubated with varying concentrations of ^{125}I anti-LIBS2 in the presence or absence of 1 mM RGDS. Bound ^{125}I-anti-LIBS2 was estimated as described under "Experimental Procedures." The *inset* shows a Scatchard (53) replot of the same data. All *lines* are the best fits of the data as estimated by use of LIGAND (54). *B*, suspensions of washed platelets (2.5×10^8/ml) were incubated with 300 nM ^{125}I-labeled Fg in the presence of varying concentrations of anti-LIBS2 Fab. The Fg bound to platelet $\alpha_{IIb}\beta_3$ was quantified as described. The values were corrected for recovery of $\alpha_{IIb}\beta_3$ by measuring the binding of the anti-β_3 antibody, mAb15, in parallel.

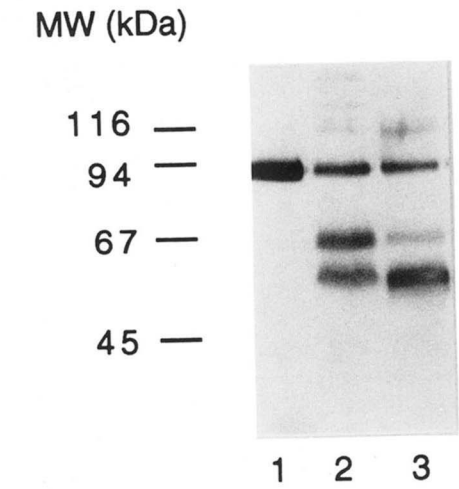

FIG. 2. **Localization of the anti-LIBS2 epitope in chymotryptic fragments of β_3.** Platelets were digested with 500 μg chymotrypsin/ml for 0 (*lane 1*), 1 (*lane 2*), or 4 (*lane 3*) h. Following solubilization of platelet proteins, SDS-polyacrylamide gel electrophoresis, and transfer to nitrocellulose, the blots were reacted with the anti-LIBS2 antibody as described under "Experimental Procedures."

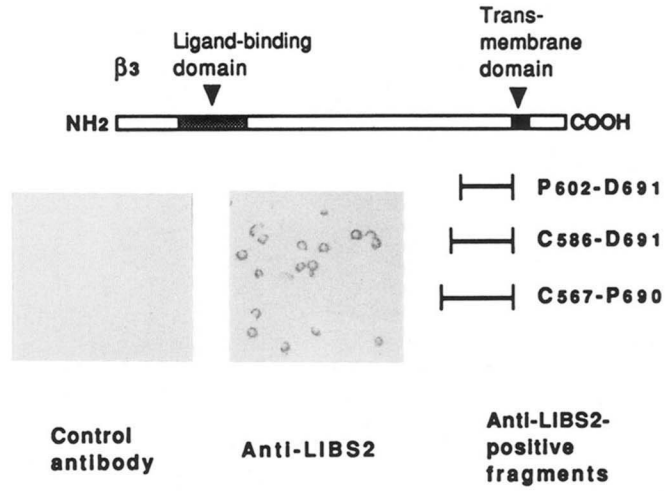

FIG. 3. **Localization of the anti-LIBS2 epitope by use of a β_3 cDNA fragment library.** The library was screened by creating a replica of a plate containing phage- infected *E. coli* Y1090 cells on nitrocellulose membranes. Following treatment with IPTG, the membrane was incubated with anti-LIBS2 antibody, biotinylated rabbit anti-mouse IgG, and followed by a peroxidase-conjugated avidin-biotin complex. Positive clones were subcloned by polymerase chain reaction into a TA vector (Invitrogen, San Diego, CA), and their sequence was determined by dideoxy sequencing (30). *Inset*, the recombinant λgt11-isolated plaques react with anti-LIBS2 and not with a control monoclonal antibody.

ferred onto nitrocellulose membranes. The nucleotide sequences of three DNA clones recovered from positive plaques encoded overlapping sequences that included 89 amino acid residues of β_3 spanning P602-P690. This sequence is located immediately amino-terminal to the predicted transmembrane domain (Fig. 3).

To verify the location of the anti-LIBS2 epitope, the P602-P690 fragment was inserted into the pMALcRI vector and expressed as a fusion protein with the *E. coli* MBP. By immunoblotting, the fusion protein contained the anti-LIBS2 epitope (Fig. 4, *inset*). In addition, to confirm that P602-P690 contains the relevant epitope for the functional effects of anti-LIBS2, we examined the effect of the fusion protein on anti-LIBS2-induced platelet aggregation. Anti-LIBS2 (1 μM) induced prompt aggregation of platelets without antecedent shape change (Fig. 4). Addition of fusion protein at 8 μM blocked anti-LIBS2-induced platelet aggregation, but not aggregation induced by another anti β_3 monoclonal antibody, anti-LIBS6 (Fig. 4). Maltose-binding protein alone (8 μM) was without effect on anti-LIBS2-induced aggregation.

To localize the anti-LIBS2 epitope within the P602-P690 sequence, we synthesized a series of 11 overlapping 11–15 residue peptides comprising the entire sequence of the region (Fig. 5). None of these peptides, at concentrations as high as 5 mM, inhibited the binding of anti-LIBS to purified $\alpha_{IIb}\beta_3$. Moreover, anti-LIBS2 failed to bind to any of these peptides immobilized on the wells of microtiter plates. We also produced fusion proteins containing truncations of the P602-P690 sequence. Deletion of the NH_2-terminal 11 or COOH-terminal 23 residues in the recombinant fusion protein also resulted in loss of reactivity in immunoblots. Taken together, these data suggest that the anti-LIBS2 epitope is a topographic determinant that can be assembled in an 89-residue fragment of β_3.

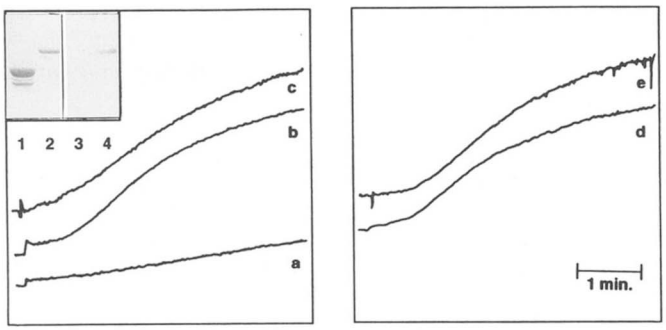

FIG. 4. **Inhibition of anti-LIBS2-induced platelet aggregation by the recombinant anti-LIBS2 epitope.** The cDNA fragment containing the anti-LIBS2 epitope was subcloned into pMALc RI expression vector and subsequently the fusion protein was isolated as described under "Experimental Procedures." *a–c*, platelet aggregation induced by anti-LIBS2. *d* and *e*, platelet aggregation induced by anti-LIBS6. *a* and *d*, no inhibitor added. *b* and *e*, 0.25 mg/ml of P602–690 MBP fusion protein was added. *c*, 0.25 mg/ml MBP was added. *Inset*, Coomassie Blue stain (*lanes 1* and *2*) and immunoblots with anti-LIBS2 (*lanes 3* and *4*) showing purified MBP (*lanes 1* and *3*) and purified P602-P690 MBP fusion protein (*lanes 2* and *4*).

The P602-P690 sequence contains 9 cysteines, suggesting that disulfide bonding could be involved in the assembly of this discontinuous determinant. Indeed, reduction of $\alpha_{IIb}\beta_3$ or reduction-alkylation of the fusion protein resulted in loss of their reactivity with anti-LIBS2 (not shown). Of the cysteines in this fragment, Cys^{631} and Cys^{655} form disulfide bonds with cysteines located outside of the P602-P690 sequence (41), and thus cannot contribute to the natural disulfide bonds responsible for the formation of the epitope in the fusion protein. Cys^{635} and Cys^{633} form a disulfide bond, but these 2 cysteines were not eliminated by deletion of the NH_2-terminal 11 or COOH-terminal 23 residues of the fragment. Cys^{687} is reported to form a long range disulfide bond with 1 of the 4 cysteines at the NH_2-terminal end (Cys^{604}, Cys^{608}, Cys^{614}, and Cys^{617}), which would be disrupted by removal of either the NH_2-terminal or COOH-terminal end of the fragment. Nevertheless, a $Cys^{687} \rightarrow$ Ser mutant still bound anti-LIBS2 (Fig. 5) indicating that such a disulfide bond is not essential for preservation of the epitope.

Examination of the Spatial Relationship of Anti-LIBS2-binding Site and Ligand-binding Site by Electron Microscopy—The proposed ligand-binding site of $\alpha_{IIb}\beta_3$ includes residues 109–171 (39) and 211–222 (40) in β_3. However, the anti-LIBS2 epitope, located in the 609–690 region of β_3, is considerably distant from the known ligand-binding sites in the primary structure. To assess directly the spatial relationship between the ligand-binding domain and the COOH-terminal Pro^{602}-Pro^{690} region, the anti-LIBS2-binding site was localized by electron microscopy of rotary shadowed antibody-$\alpha_{IIb}\beta_3$ complexes.

When viewed by electron microscopy, rotary shadowed $\alpha_{IIb}\beta_3$ consists of a globular head, to which Fg binds (34), and two tails containing the COOH-terminal regions of α_{IIb} and possibly β_3, respectively. In 90% of images, anti-LIBS2, with the characteristic Y-shape of an IgG, was bound to one of the tails of $\alpha_{IIb}\beta_3$ (Fig. 6). The distance between anti-LIBS2-binding site and the globular head was 8 ± 3 nm (the average total length of the tail is approximately 18 nm). The ligand-binding site is on the side of the globular head about 8 nm from the head-tail junction. Thus, the total distance between the anti-LIBS2 determinant and the ligand-binding site would be 13 to 19 nm. In images containing both bound anti-LIBS2 and bound Fg, the distance between the antibody-binding site and the ligand-binding site was about 16 nm, in agreement

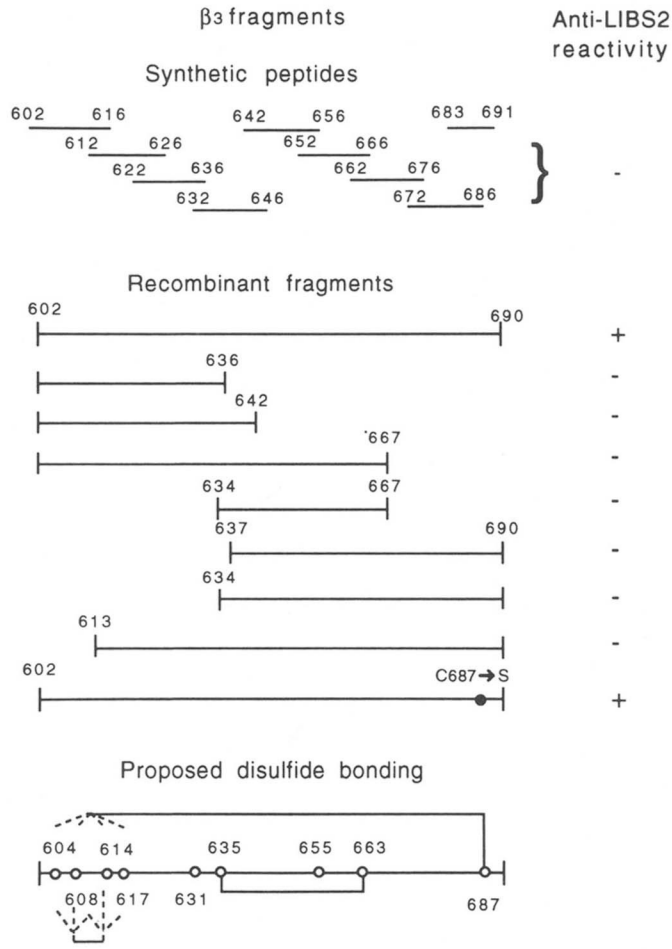

FIG. 5. **Reaction of anti-LIBS2 with synthetic peptides and MBP fusion proteins containing β_3 fragments.** Reactivity of anti-LIBS2 with synthetic peptides was assessed by measurement of the direct binding of antibody to peptide-coated wells, and by the capacity of the peptides to inhibit anti-LIBS2 binding to plates coated with $\alpha_{IIb}\beta_3$ as described under "Experimental Procedures." Reactivity with fusion proteins was detected by immunoblotting, as also described under "Experimental Procedures." The proposed disulfide bonds based on the work of Calvete *et al.*(41) are (*a*) a bond between Cys residues in the Cys^{602}-Cys^{617} region; (*b*) Cys^{687} to one of the cysteine residues between 602–617; *c*, Cys^{635}-Cys^{663}.

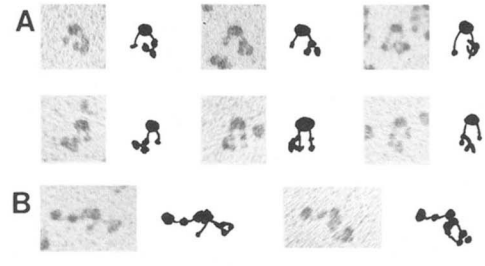

FIG. 6. **Electron microscope images of anti-LIBS2 binding to integrin $\alpha_{IIb}\beta_3$ showing that anti-LIBS2 binds to the COOH-terminal portion of one of the tails.** The first set of panels illustrates typical Y-shaped anti-LIBS2 bound to $\alpha_{IIb}\beta_3$. Tracings of the molecule are shown to the right. The *lower panels* illustrate anti-LIBS2 bound to $\alpha_{IIb}\beta_3$ that is interacting with a Fg molecule. Note the typical tri-nodular Fg molecule interacting through one of its distal nodular domains with the globular head of $\alpha_{IIb}\beta_3$. The anti-LIBS2 is bound to one of the tails, about 16 nm from the site of Fg binding.

with the previous calculation. This distance indicates that the cooperative binding of ligand and anti-LIBS2 is a result of a propagated long distance conformational rearrangement.

DISCUSSION

The major findings of this study are (*a*) the anti-LIBS2 antibody and ligands (Fg and Fg-mimetic peptides) bind cooperatively to integrin $\alpha_{IIb}\beta_3$. This indicates a linkage between the ligand-binding site and the antibody-binding site in the integrin. (*b*) The anti-LIBS2-binding site is located within an 89-residue stretch immediately adjacent to the transmembrane domain of the β_3 subunit. (*c*) The ligand-binding site and anti-LIBS3-binding site are separated by about 16 nm in the three-dimensional structure of integrin $\alpha_{IIB}\beta_3$. This indicates that conformational changes can propagate over long distance in this integrin. Such changes are likely to be involved in the bidirectional signaling function of this integral membrane protein.

The cooperativity of ligand and anti-LIBS2 binding to $\alpha_{IIb}\beta_3$ directly indicates a conformational link between their binding sites. In particular, a quantitative analysis of anti-LIBS2 binding in the presence and absence of ligand established that the ligand increases the affinity of anti-LIBS2 binding by about 20-fold, but does not influence the number of LIBS2-binding sites. Previous work identified monoclonal anti-β_3 antibodies that increase Fg binding to integrin $\alpha_{IIb}\beta_3$ (4, 18, 19). Conversely, Fg and Fg-mimetic peptides promoted the binding of these anti-β_3 antibodies (4, 18, 19). Nevertheless, one study reported that activating antibody bound with high affinity to only a small number of binding sites on platelets (19) and that the effect of an RGD peptide ligand was to increase the number of antibody-binding sites. Such findings suggest that the antibody bound to a subpopulation of $\alpha_{IIb}\beta_3$ and increased the ligand binding affinity of other receptors via an amplification mechanism. In contrast, our results, obtained with the anti-LIBS2, favor a cooperative interaction. This mechanism is also suggested by the capacity of anti-LIBS2 to enhance the affinity of Fg binding to highly purified $\alpha_{IIb}\beta_3$, precluding amplification by accessory molecules. Thus, the binding of ligand to $\alpha_{IIb}\beta_3$ results in a conformational change which is propagated to the LIBS2-binding site. Conversely, the binding of anti-LIBS2 to the receptor results in a conformational rearrangement propagated to the ligand-binding site.

The anti-LIBS2-binding site is located within an 89-amino-acid region immediately NH_2-terminal to the transmembrane domain of β_3. This conclusion is based on the reactivity of the recombinant fusion protein containing this sequence with anti-LIBS2. It is possible that a second binding site for anti-LIBS2 may exist on β_3. This appears unlikely because the estimated number of anti-LIBS2-binding sites closely approximated the estimated number of sites for other anti-$\alpha_{IIb}\beta_3$ antibodies (42). Second, proteolytic mapping of the native protein also supported the separation of the ligand-binding site and the anti-LIBS2-binding site. The disulfide bonding pattern of the 56 cysteines of β_3 has been partially elucidated (41). The anti-LIBS2 epitope was sensitive to reduction, suggesting that its formation is dependent on the integrity of certain of these disulfide bonds. In the present study, deletions of 11 residues from the NH_2 terminus or 22 residues from the COOH terminus of the 89-residue fragment resulted in a loss of reactivity. These findings, along with the disulfide dependence, suggest that the anti-LIBS2 epitope is discontinuous. Nevertheless, the 9 cysteines contained in the P602–690 fragment can pair correctly to form the epitope *in vitro*. Moreover, Cys^{687}, which forms a long range disulfide to the NH_2-terminal region of this fragment, was not essential for formation of the epitope. Thus, the anti-LIBS2 antibody appears to bind to a unique discontinuous epitope located immediately adjacent to the transmembrane domain of β_3.

The anti-LIBS2-binding site is ~16 nm distant from the Fg-binding site in $\alpha_{IIb}\beta_3$. This conclusion is based on direct viewing of the ternary complex of Fg, the antibody, and the integrin. Previous studies have provided rotary shadowing images of integrins as 8 × 12-nm globular heads with two 18-nm tails projecting from them (34, 43, 44). These images led to molecular models in which the ligand-binding site was proposed to be a considerable distance from the plasma membrane. This model was recently confirmed by rotary shadowing electron microscopy of $\alpha_{IIb}\beta_3$ with ligands bound (34). In the present study, in virtually all of the images, anti-LIBS2 was bound to the distal portion of one of the tails of $\alpha_{IIb}\beta_3$. We never encountered images of antibody bound to both tails. Moreover, in images of the ternary complex of Fg with the antibody, a distance of ~16 nm was observed between the bound ligand and the bound antibody. Previous studies suggest that Cys^{655} forms a disulfide bond with Cys^{406} (41). Cys^{655} resides in the middle of the Pro^{602}-Pro^{690} region containing the LIBS2 epitope. It is thus possible that Cys^{655} is in close apposition to the globular head of the integrin and the 36 residues from Cys^{655} to Asp^{691} could span the distance from the head to the transmembrane domain. It is also possible that $\alpha_{IIb}\beta_3$ may undergo some spontaneous disulfide rearrangement *in vitro* (45) which may affect its three-dimensional structure. Indeed, we[2] have observed that in aged or frozen-thawed preparations of $\alpha_{IIb}\beta_3$, the tails are often seen to come into close apposition to the globular head of the molecule. In any event, the current data indicate an ~16 nm separation between the two cooperative binding sites. This implies the existence of a long range conformational transition in the protein.

The helical conformation of the intramembrane segments of many transmembrane proteins probably precludes linear propagation of conformational changes (46). Nevertheless, transmembrane receptors can transmit signals through lateral interactions (47). In contrast, receptors with multiple transmembrane domains could transmit signals through intramolecular rearrangements, without need for lateral interactions (48). For example, in a truncated soluble bacterial aspartate receptor, ligand binding 60 Å from the membrane surface resulted in a 1.4-Å shift in the relationship of helices proximal to the membrane-spanning segment (13). Similarly, integrin $\alpha_{IIb}\beta_3$ has two membrane-spanning subunits (49, 50). Intracellular signals may be directed through integrin cytoplasmic domains (51, 52) and ultimately result in changes in the conformation of the extracellular domain of this integrin. In the present study, an antibody, whose epitope is immediately adjacent to the transmembrane domain, bound cooperatively with ligand. Given the ~16 nm distance between the anti-LIBS2 epitope and the ligand-binding site, this cooperativity indicates a long range conformational change in this transmembrane protein *in situ*. Moreover, this suggests that physiological signals initiated by interactions at the integrin cytoplasmic domain (51, 52) could be propagated to the ligand-binding site.

REFERENCES

1. Bennett, J. S., and Vilaire, G. (1979) *J. Clin. Invest.* **64**, 1393–1401
2. Marguerie, G. A., Plow, E. F., and Edgington, T. S. (1979) *J. Biol. Chem.* **254**, 5357–5363
3. Sims, P. J., Ginsberg, M. H., Plow, E. F., and Shattil, S. J. (1991) *J. Biol. Chem.* **266**, 7345–7352
4. O'Toole, T. E., Loftus, J. C., Du, X., Glass, A. A., Ruggeri, Z. M., Shattil,

[2] J. Weisel, unpublished observations.

S. J., Plow, E. F., and Ginsberg, M. H. (1990) *Cell Regulation* **1,** 883–893
5. Ginsberg, M. H., Du, X., and Plow, E. F. (1992) *Curr. Opin. Cell Biol.* **4,** 766–771
6. Dustin, M. L., and Springer, T. A. (1989) *Nature* **341,** 619–624
7. Frelinger, A. L., III, Cohen, I., Plow, E. F., Smith, M. A., Roberts, J., Lam, S. C.-T., and Ginsberg, M. H. (1990) *J. Biol. Chem.* **265,** 6346–6352
8. Shattil, S. J., and Brugge, J. S. (1991) *Curr. Opin. Cell Biol.* **3,** 869–879
9. Pilch, P. F., and Czech, M. P. (1980) *Science* **210,** 1152–1153
10. Falke, J. J., and Koshland, D. E., Jr. (1987) *Science* **237,** 1596–1600
11. Metzger, H. (1983) *Contemp. Top. Mol. Immunol.* **9,** 115–145
12. Baron, V., Gautier, N., Komoriya, A., Hainaut, P., Scimeca, J-C., Mervic, M., Lavielle, S., Dolais-Kitabgi, J., and Van Obberghen, E. (1990) *Biochemistry* **29,** 4634–4641
13. Milburn, M. V., Prive, G. G., Milligan, D. L., Scott, W. G., Yeh, J., Jancarik, J., Koshland, D. E., Jr., and Kim, S-H. (1991) *Science* **2254,** 1342–1347
14. Parise, L. V., Helgerson, S. L., Steiner, B., Nannizzi, L., and Phillips, D. R. (1987) *J. Biol. Chem.* **262,** 12597–12602
15. Greenfield, C., Hiles, I., Waterfield, M. D., Federwisch, M., Wollmer, A., Blundell, T. L., and McDonald, N. (1989) *EMBO J.* **8,** 4115–4123
16. Donner, D. B., and Yonkers, K. (1983) *J. Biol. Chem.* **258,** 9413–9418
17. Frelinger, A. L., III, Lam, S. C-T., Plow, E. F., Smith, M. A., Loftus, J. C., and Ginsberg, M. H. (1988) *J. Biol. Chem.* **263,** 12397–12402
18. Frelinger, A. L., III, Du, X., Plow, E. F., and Ginsberg, M. H. (1991) *J. Biol. Chem.* **266,** 17106–17111
19. Kouns, W. C., Wall, C. D., White, M. M., Fox, C. F., and Jennings, L. K. (1990) *J. Biol. Chem.* **265,** 20594–20601
20. Plow, E. F., and Ginsberg, M. H. (1981) *J. Biol. Chem.* **256,** 9477–9482
21. Shattil, S. J., Hoxie, J. A., Cunningham, M., and Brass, L. F. (1985) *J. Biol. Chem.* **260,** 11107–11114
22. Bajt, M. L., Ginsberg, M. H., Frelinger, A. L., III, Berndt, M. C., and Loftus, J. C. (1992) *J. Biol. Chem.* **267,** 3789–3794
23. Loftus, J. C., O'Toole, T. E., Plow, E. F., Glass, A., Frelinger, A. L., III, and Ginsberg, M. H. (1990) *Science* **249,** 915–918
24. Plow, E. F., Srouji, A. H., Meyer, D., Marguerie, G. A., and Ginsberg, M. H. (1984) *J. Biol. Chem.* **259,** 5388–5391
25. Ginsberg, M. H., Taylor, L., and Painter, R. G. (1980) *Blood* **55,** 661–668
26. Laemmli, U. K. (1970) *Nature* **227,** 680–685
27. Towbin, H., Staehelin, T., and Gordon, J. (1979) *Proc. Natl. Acad. Sci. U. S. A.* **76,** 4350–4354
28. Ginsberg, M. H., Loftus, J., Ryckwaert, J.-J., Pierschbacher, M. D., Pytela, R., Ruoslahti, E., and Plow, E. F. (1987) *J. Biol. Chem.* **262,** 5437–5440
29. O'Toole, T. E., Loftus, J. C., Plow, E. F., Glass, A., Harper, J. R., and Ginsberg, M. H. (1989) *Blood* **74,** 14–18
30. Sanger, F. (1981) *Science* **214,** 1205–1210
31. Gordon, T. P., Loftus, J. C., Levin, E., O'Toole, T. E., McMillan, R., Lindstrom, J., and Ginsberg, M. H. (1992) *J. Clin. Invest.* **90,** 992–999
32. Kadowaki, H., Kadowaki, T., Wondisford, F. E., and Taylor, S. I. (1989) *Gene (Amst.)* **76,** 161–166
33. Du, X., Plow, E. F., Frelinger, A. L., III, O'Toole, T. E., Loftus, J. C., and Ginsberg, M. H. (1991) *Cell* **65,** 409–416
34. Weisel, J. W., Nagaswami, C., Vilaire, G., and Bennett, J. S. (1992) *J. Biol. Chem.* **267,** 16637–16643
35. Ginsberg, M., Pierschbacher, M. D., Ruoslahti, E., Marguerie, G. A., and Plow, E. (1985) *J. Biol. Chem.* **260,** 3931–3936
36. Ruggeri, Z. M., Houghten, R. A., Russell, S. R., and Zimmerman, T. S. (1986) *Proc. Natl. Acad. Sci. U. S. A.* **83,** 5708–5712
37. Lam, S. C.-T., Plow, E. F., Smith, M. A., Andrieux, A., Ryckwaert, J.-J., Marguerie, G., and Ginsberg, M. H. (1987) *J. Biol. Chem.* **262,** 947–950
38. Niewiarowski, S., Norton, K. J., Eckardt, A., Lukasiewicz, H., Holt, J. C., and Kornecki, E. (1989) *Biochim. Biophys. Acta* **983,** 91–99
39. D'Souza, S. E., Ginsberg, M. H., Burke, T. A., Lam, S. C.-T., and Plow, E. F. (1988) *Science* **242,** 91–93
40. Charo, I. F., Nannizzi, L., Phillips, D. R., Hsu, M. A., and Scarborough, R. M. (1991) *J. Biol. Chem.* **266,** 1415–1421
41. Calvete, J. J., Henschen, A., and Gonzalez-Rodriguez, J. (1991) *Biochem. J.* **274,** 63–71
42. McEver, R. P., Baenziger, N. L., and Majerus, P. W. (1980) *J. Clin. Invest.* **66,** 1311–1318
43. Carrell, N. A., Fitzgerald, L. A., Steiner, B., Erickson, H. P., and Phillips, D. R. (1985) *J. Biol. Chem.* **260,** 1743–1749
44. Nermut, M. V., Green, N. M., Eason, P., Yamada, S. S., and Yamada, K. M. (1988) *EMBO J.* **7,** 4093–4099
45. Phillips, D. R., and Agin, P. P. (1977) *J. Biol. Chem.* **252,** 2121–2126
46. Singer, S. J. (1990) *Annu. Rev. Cell Biol.* **6,** 247–296
47. Yarden, Y., and Schlessinger, J. (1987) *Biochemistry* **26,** 1443–1451
48. Robinson, P. R., Cohen, G. B., Zhukovsky, E. A., and Oprian, D. D. (1992) *Neuron* **9,** 719–725
49. Poncz, M., Eisman, R., Heidenreich, R., Silver, S. M., Vilaire, G., Surrey, S., Schwartz, E., and Bennett, J. S. (1987) *J. Biol. Chem.* **262,** 8476–8482
50. Fitzgerald, L. A., Steiner, B., Rall, S. C., Jr., Lo, S., and Phillips, D. R. (1987) *J. Biol. Chem.* **262,** 3936–3939
51. Chen, Y. P., Djaffar, I., Pidard, D., Steiner, B., Cieutat, A. M., Caen, J. P., and Rosa, J. P. (1992) *Proc. Natl. Acad. Sci. U. S. A.* **89,** 10169–10173
52. O'Toole, T. E., Mandelman, D., Forsyth, J., Shattil, S. J., Plow, E. F., and Ginsberg, M. H. (1991) *Science* **254,** 845–847
53. Scatchard, G. (1949) *Ann. N. Y. Acad. Sci.* **51,** 600–672
54. Munson, P. J., and Rodbard, D. (1980) *Anal. Biochem.* **107,** 220–239